Theory for high-T_c superconductors considering inhomogeneous charge distribution

E. V. L. de Mello, E. S. Caixeiro, and J. L. González
Departamento de Física, Universidade Federal Fluminense, av. Litorânia s/n, Niterói, R.J., 24210-340, Brazil
(Received 24 October 2001; revised manuscript received 21 October 2002; published 13 January 2003)

We propose a general theory for the dependence of the critical and pseudogap temperatures T_c and T^* on the doping concentration for high-T_c oxides, taking into account the charge inhomogeneities in the CuO_2 planes. Several recent experiments have revealed that the charge density ρ in a given compound (mostly underdoped) is intrinsic inhomogeneous with large spatial variations which leads to a local charge density $\rho(r)$. These differences in the local charge concentration yield insulator and metallic regions, either in an intrinsic granular or in a stripe morphology. In the metallic region, the inhomogeneous charge density produces also spatial or local distributions which form Cooper pairs at a local superconducting critical temperatures $T_c(r)$ and zero temperature gap $\Delta_0(r)$. For a given compound, the measured onset of the vanishing gap temperature is identified as the pseudogap temperature, that is, T^*, which is the maximum of all $T_c(r)$. Below T^*, due to the distribution of $T_c(r)$'s, there are some superconducting regions surrounded by an insulator or a metallic medium. The transition to a coherent superconducting state corresponds to the percolation threshold among the superconducting regions with different $T_c(r)$'s. The charge inhomogeneities have been studied by recent scanning tunneling microscopy experiments which provided a model for our phenomenological distribution. To make definite calculations and compare with the experimental results, we derive phase diagrams for the $Bi_2Sr_2CaCu_2O_{8+x}$ (Bi2212), $La_{2-x}Sr_xCuO_4$ (LSCO), and $YBa_2Cu_3O_{7-y}$ (YBCO) families, with a mean field theory for superconductivity using an extended Hubbard Hamiltonian. We show also that this approach provides insights into several experimental features of high-T_c oxides.

DOI: 10.1103/PhysRevB.67.024502 PACS number(s): 74.72.−h, 74.20.−z, 74.81.−g, 71.38.−k

I. INTRODUCTION

It is well known that the properties of high-temperature superconductors (HTSC's) vary in an unusual way when a moderate density of holes are introduced into the CuO_2 planes by chemical doping. This is one of the reasons why, despite large experimental and theoretical efforts, the nature of the superconductivity in these materials remains to be explained.[1] Correlations show the parent undoped compound to be a Mott insulator and, upon doping, the underdoped compounds display unusual metallic properties with increasing T_c. Doping beyond the optimal level yields normal metals with Fermi liquid behavior and with decreasing T_c.

The unusual properties of underdoped samples have motivated several experiments, and two features have been discovered which distinguish them from the overdoped compounds: first, the appearance of a pseudogap at a temperature T^*, that is, a discrete structure of the energy spectrum above T_c, identified by several different probes.[2] T^* was also found to be present in overdoped samples,[2,3] but at temperatures near T_c. Second, there is increasing evidence that electrical charges are highly inhomogeneous up to (and even further) the optimally doped region.[4–9] These charge inhomogeneities are due neither to impurities nor to crystal defects, but are intrinsic to the type of cuprate, producing local lattice distortions in the CuO_2 bond length.[10] In fact, such intrinsic inhomogeneities are also consistent with the presence of charge domains either in a granular[7–9] or a stripe[11–13] form.

Therefore, in our view, it is very likely that the pseudogap and the intrinsic charge inhomogeneities are closely related, and understanding their interplay is of great importance to understanding the general phenomenology and the phase diagrams of the HTSC families. Currently there are two main different proposals to explain the existence of the pseudogap: In the first one, the pseudogap is regarded as a normal state precursor of the superconducting gap due to local dynamic pairing correlations in a state without long range phase coherence, and T_c is much smaller than T^* because of strong phase fluctuations.[14,15] In the second proposal, the pseudogap is a normal state gap, which is necessarily independent of the superconducting gap, and which competes with the superconductivity, existing even below T_c for compounds around the optimum doping, ending in a quantum critical point[16–18] at zero temperature.

Recently we described a simple scenario[19]: when the temperature of a given sample is decreasing and reaches T^*, it activates the formation of pairs at some selected low doping metallic regions. Initially these superconducting or pair-rich regions are not connected and there is no phase coherence over the whole system. The coherent superconducting transition occurs when the temperature reaches a value (T_c) at which the different superconducting regions percolate. This scenario relies heavily upon the fact that the cuprates have an intrinsic inhomogeneous charge distribution. Thus a given HTSC compound with an average hole per Cu ion density $\langle\rho\rangle$ and with an inhomogeneous microscopic charge distribution $\rho(r)$ has a distribution of small clusters or stripes with a given local $T_c(r)$ ($0<\langle\rho\rangle\leqslant 1$ and $0<\rho(r)\leqslant 1$). Thus the model depends strongly on the intrinsic charge distribution $\rho(r)$ although their exact form is not well known, and since the discovery of the spin-charge stripes,[11] they are a matter of intense current research. As a consequence, several recent experiments demonstrated that the charge distributions are more inhomogeneous for underdoped compounds and more

homogeneous for overdoped compounds, and may resemble either a granular[4–9] or a stripe structure.

In the spin-charge striped scenario, some regions of the plane are heavily doped (the stripes) and other regions are underdoped, filling the space between the charge-rich stripes. Stripe phases occur due to the antiferromagnetic interaction among magnetic ions and Coulomb interaction between the charges, both of which favor localization. On the other hand, the zero-point motion of the holes favors delocalization, and tends to create phase-separated states rich either in spin or charge. Experimentally, stripes are more easily detected in insulating materials, where they are static, but there is evidence of fluctuating stripe correlations in metallic and superconducting compounds.[12,11,13]

Based on the results of the above mentioned experiments, we have introduced a local charge distribution $\rho(r)$ to model the real charge distributions inside a HTSC compound. Since doping produces an intrinsic inhomogeneous charge distribution and metallic and insulator regions seem to coexist, we assume that it contains two parts: one for a hole-rich partition and the other for a hole-poor partition. This mimics the striped phases. The hole-poor regions are, in most cases, antiferromagnetic Mott insulators. The hole-rich regions form an inhomogeneous metal with a spatially varying charge density. The existence of the intrinsic charge inhomogeneities have several consequences, and one of them is the non-Fermi-liquid behavior of the underdoped compounds. As concerns the superconductivity, they produce spatially dependent superconducting gaps $\Delta_{sc}(r)$ due to the short coherence length, and also spatially dependent superconducting domains with a critical temperatures $T_c(r)$. Recently, very fine scanning tunneling microscopy/spectroscopy (STM/S) data[7,8] has revealed the spatial variation through the differential conductance which provides a strong evidence for such distribution of zero temperature superconducting gap $\Delta_{sc}(r)$. More recently, STM data on Bi2212, using scattering resonances at Ni impurity atoms, revealed a large nanoscale spatial dependence of the superconducting gap.[9]

All together, these experiments show variations on local density of states (LDOS) of just a few Å. This is consistent with the very short coherence length in HTSC. Since $T_c(r)$ is proportional to $\Delta_{sc}(r)$, the opening of the largest gap occurs at the highest of all the $T_c(r)$'s, which is exactly T^*. Above T^* there is no gap and, below it, there is the development of some superconducting clusters inside the material. Depending on the distribution of the values of $T_c(r)$ in the compound, some regions become superconducting. Decreasing the temperature, the number of superconducting clusters increases, bringing about the superconducting domains to grow. When the temperature reaches a value which is the T_c of the compound, the superconducting regions percolate through the sample and therefore it can hold a dissipationless current.

In Fig. 1 we show a schematic local charge density distribution $\rho(r)$ which is based on the above experimental data, as mentioned, and could give rise to a gap distribution of $\Delta_{sc}(r)$. This is a pictorial sketch of what should be the real charge distribution for a optimal doped HTSC, based on the above information. It reflects the nanoscale variations of the superconducting energy gap or the nanoscale variations on the density of charges in the material.

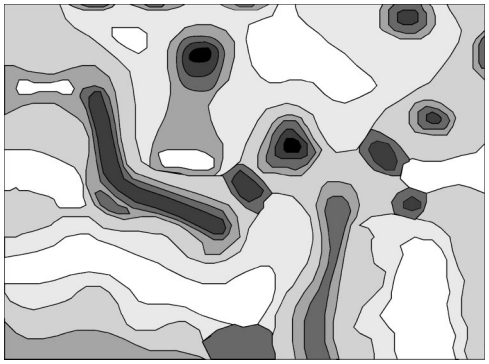

FIG. 1. Sketch of the possible charge distribution in a HTSC compound. The white part represents the insulator or hole-poor regions. The gray regions mimics the hole-rich metallic part of the compound. The lighter regions are for metals with higher values of the superconducting gap and the darker regions is for lower gap regions.

This percolating scenario can be understood by analyzing the scanning superconducting quantum inference device microscopy magnetic data, which makes a map of the expelled magnetic flux (Meissner effect) domains on LSCO films.[20] This experiment shows the regions where the Meissner effect continuously develops from near T^* to temperatures well below the percolating threshold T_c. Notice that the regions without magnetic flux due to the Meissner effect can exist only where the Cooper pairs are in phase coherence in a large spatial region. Furthermore there is no apparent difference, other than the size of the superconducting region, as the temperature changes across T_c. Second, it shows the existence of the superconducting regions above T_c which differ only in size from those below T_c. Furthermore, the *d*-wave nature of both pseudogap and order parameters and the tunneling conductance and angle-resolved photoemission spectroscopy (ARPES) measurements,[2] with their curves evolving smoothly across T_c, are compelling evidence in favor of a similar nature of both gap and pseudogap.

Several different ideas of a superconducting phase in cuprates attainable by some form of percolation between pairs, clusters' or stripes are not new.[21–23] More recently, a percolating approach was suggested and supported by a microscopic model based on a spatially dependent critical temperature $T_c(r)$ due to intrinsic inhomogeneities like pair breakers or spatial dependence of the superconducting coupling constant proposed by Ovchinnikov *et al.*[24] They derived the density of states due to the spatial distribution of coupling constants. A different method based on the bond percolation between pre-formed mesoscopic Jahn-Teller pairs was proposed recently[25] as a mechanism to attain a superconducting phase coherence . On the other hand, the spatial variations on the LDOS due to charge disorder were taken into account in calculations using a generalized *t-J* model.[26] In fact, new trends and ideas have been used to describe the effects of the intrinsic disorder and the possibility of a percolating phase not only for HTSC's but also for manganites.[27]

The ideas described in the above paragraph are on the same lines as the scenario that we want to discuss to explain why the occurrence of pairing and the phase coherent superconducting state in the high-T_c superconductors appears to occur independently: we show that the percolation theory, i.e., that the superconducting state is reached through the percolation of regions rich in preformed pairs which provides good quantitative agreement with the measured T^* and T_c phase diagrams. Notice that there is a general agreement with respect to the experimental $T_c(\langle\rho\rangle)$ curves, since most of them are obtained through the same method, namely, resistivity measurements. However the measured values of T^* found in the literature are obtained through different methods and seems to vary considerably, depending on the specific experimental probe used.[2] Such difference may be due to the anisotropic d-wave nature of the gap amplitude and the fact that a given experimental technique is sensitive to excitations at a particular wavevector magnitude. Therefore, it is natural that ARPES, tunneling spectroscopy, transport properties such as dc resistivity and optical conductivity, NMR, Knight shift relaxation rate, electronic Raman, magnetic neutron scattering, specific heat,[2,16] and recent vortexlike Nernst signal measurements[28] yield different values for the onset of vanishing gap temperature T^*. Since the origin of the charges inhomogeneities are not known, T^* could be also dependent on the way a given sample is made.

We must also emphasize that the percolating approach is not only suitable to yield good quantitative agreement with the HTSC phase diagrams but, and perhaps more importantly, it provides interesting physical insights into a number of phenomena detected in these materials: the variation of the measured pseudogap magnitude with the temperature,[2] the decreasing of the zero temperature superconducting gap Δ_0 while T_c increases for underdoped compounds,[3,29] the downturn of the linear dependence of the resistivity with the temperature for underdoped samples and the increase of Hall carriers with the temperature, mostly measured for the optimally doped and underdoped compounds,[30] the downturn of the linear specific heat coefficient, etc. These properties will be discussed in more detail in Sec. IV.

This paper is divided as follows: in Sec. II, we introduce the charge distributions appropriate to mimic the real charge distribution inside the material and reproduce the T^* and T_c phase diagrams. In Sec. III, we derive the phase diagram for Bi2212, LSCO, and YBCO, and make a comparison with the experimental data. We use a mean field BCS-like method with an extended Hubbard Hamiltonian to derive the onset of vanishing gap at T^*, but it should be emphasized that the percolating approach introduced here is independent of any method of calculating the superconducting pair formation. In Sec. IV, we comment on the applications and implications of the percolation theory to several physical properties of HTSC's and we finish with the conclusions in Sec. V.

II. CHARGE DISTRIBUTION

The consequence of the microscopic charge inhomogeneities distribution in the CuO_2 planes, either in a striped or in a granular configuration, is the existence of domain walls between the two phases which are spontaneously created in the planes[11–13]: regions which are heavily doped or hole rich may form stripes, and other regions which are hole poor are created between these charge-rich stripes. The exactly form of these charge distributions is not well known, but we can obtain insights from a number of recent experiments. Neutron powder diffraction[5,6,10] suggests that charge inhomogeneities modify the Cu-O bond length, leading to a distribution of bond lengths for optimal and underdoped compounds. Scanning tunneling microscopy/spectroscopy (STM/S) (Refs. 7 and 8) on optimally doped $Bi_2Sr_2CaCu_2O_{8+x}$ measures nanoscale spatial variations in the local density of states and the superconducting gap at a very short length scale of ≈ 14 Å. These results suggest that, instead of a single value, the zero temperature superconducting gap assumes different values at different spatial locations in the crystal, and their statistics yield a Gaussian distribution.[8] High resolution STM measurements[9] revealed an interesting map of the superconducting gap spatial variation for underdoped Bi2212. Their data are compatible, as they pointed out, with a granular superconducting grains separated by non-superconducting regions. Based on their measured gap histogram [see Fig. 4(b) of Lang *et al.*[9]] and on similar data of Pan *et al.*,[8] we can draw some insights on the real charge distribution inside a HTSC.

Thus, in order to model the above experimental observations and to be capable of performing calculations which may reproduce the measured phase diagrams, namely, T^* and T_c for a given family of compounds, we used a combination of a Poisson and a Gaussian distribution for the charge distribution $\rho(r)$. In fact, each type of distribution has a convenient property which we use below: The width of a Gaussian distribution is easy to control, and expresses the degree of disorder, but since it is symmetric it would imply in a rather small width to the low density compounds. On the other hand, a Poisson distribution starts sharply and has a long tail, which is convenient in order to deal with these these low density compounds with their experimentally measured large degree of inhomogeneities. Thus, for a given compound with an average charge density $\langle\rho\rangle$, the hole distribution $P(\rho;\langle\rho\rangle)$ or simply $P(\rho)$ is a histogram of the probability of the local hole density ρ inside the sample, separated into two branches or domains. The low density branch represents the hole-poor or nonconducting regions, and the high density one represents the hole-rich or metallic regions. As concerns the superconductivity, only the properties of the hole rich branch are important since the current flows only through the metallic region.

Such normalized charge probability distribution may be given by

$$P(\rho)=(\rho_c-\rho)\exp[-(\rho-\rho_c)^2/2(\sigma_-)^2]/\{(\sigma_-)^2 \times[2-\exp(-(\rho_c)^2/2(\sigma_-)^2)]\} \quad \text{for} \quad 0<\rho<\rho_c \tag{1}$$

$$P(\rho)=0 \quad \text{for} \quad \rho_c<\rho<\rho_m \tag{2}$$

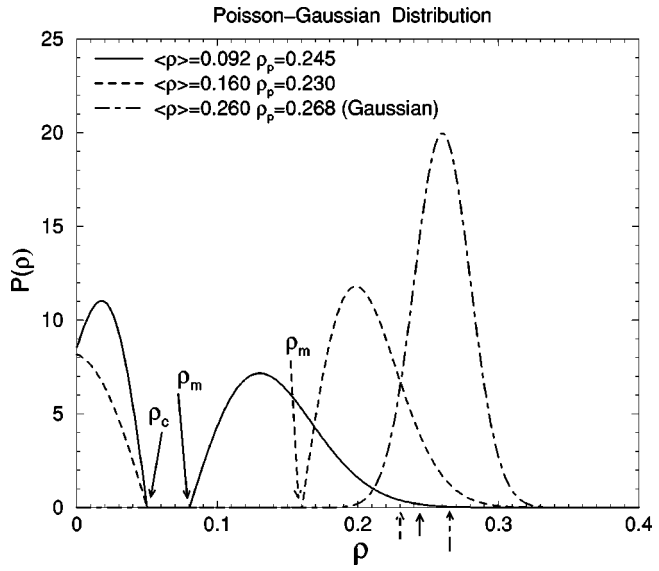

FIG. 2. Model charge distribution for the inhomogeneities or stripe two phase regions. The low density insulating (antiferromagnetic) branch is near $\rho=0$. The high density hole-rich region starts at the compound average density ρ_m which are indicated by long arrows for some selected compounds. ρ_p, indicated by the short arrows, is the density where percolation can occur.

$$P(\rho)=(\rho-\rho_m)\exp[-(\rho-\rho_m)^2/2(\sigma_+)^2]/\{(\sigma_+)^2 \times[2-\exp(-(\rho_c)^2/2(\sigma_-)^2)]\} \quad \text{for} \quad \rho_m<\rho \tag{3}$$

The value of σ_- (σ_+) controls the width of the low (high) density branch. Here ρ_c is the end local density of the hole-poor branch. ρ_m is the starting local density of the hole-rich or metallic branch. Both ρ_c and ρ_m are shown in Fig. 2 for particular cases. Each compound will have a its value of ρ_m. Thus a compound having regions with different hole concentrations which are distributed according to the above probability density function $P(\rho)$, has an average value which depends on the parameters of the distribution. We can show that the average value of the charge density is

$$\langle\rho\rangle=[\sigma_+ sqrt(\pi/2)+\rho_m+\rho_c-\sigma_- sqrt(\pi/2) \times \text{erfunction}(\rho_c/sqrt(\pi/2))]/ \times\{(\sigma_+)^2[2-\exp(-(\rho_c)^2/2(\sigma_-)^2)]\}, \tag{4}$$

here erfunction is the error function. For most compounds, due to the small values of σ_+, $\langle\rho\rangle\approx\rho_m$; see Table I below. Indeed, for a compound with average density $\langle\rho\rangle$, the values of $\sigma_\pm$ are chosen in order that percolation in the hole-rich branch occurs at a given density called ρ_p.

As the doping level $\langle\rho\rangle$ increases, the compounds become more homogeneous and therefore, we take larger values of σ_- and smaller values of the metallic branch width σ_+. We take $\rho_c\approx0.05$ as the end of the low branch because it corresponds to the onset of superconductivity to mostly cuprates. However, $\rho_c\approx0.1$ for the Bi2212 family. During the preparation of this work, we discovered that the charge probability distribution for the metallic branch, introduced as an ansatz in the beginning of our calculations, but based on the results of Pan *et al.*,[8] was confirmed by the very fine STM measurements of Lang *et al.*[9] They measured the gap probability distribution which has a Gaussian form but with a long tail which is more characteristic of a Poisson type distribution. Since there is not any experimental measurements for the hole-poor branch, σ_- is just a free parameter.

TABLE I. Some selected parameters for different doping level compounds. Notice that they are characterized by the average hole density $\langle\rho\rangle$ given in the fourth column. Notice also that the values of the metallic branch width σ_+ decreases with $\langle\rho\rangle$, showing that the degree of disorder decrease with the doping. The * marks the distributions plotted in Fig. 2. The value of $\sigma_+=0.04$ for $\langle\rho\rangle=0.16$ is taken from the experimental data of Pan *et al.* (Ref. 8).

ρ_m	σ_-	σ_+	$\langle\rho\rangle$	ρ_p
0.080*	0.033	0.050	0.09	0.245
0.100	0.034	0.050	0.10	0.240
0.120	0.037	0.050	0.12	0.238
0.160*	0.057	0.040	0.16	0.230
0.200	0.090	0.026	0.20	0.239
0.220	0.097	0.017	0.22	0.245
0.260*	0.04(G)	0.04(G)	0.26	0.268

We can obtain a reliable estimation of the σ_+ values from the experimental STM/S Gaussian histogram distribution for the local gap[8] in an optimally doped $Bi_2Sr_2CaCu_2O_{8+x}$ ($\rho_m\approx0.32$). From Fig. 2(d) of Ref. 7, one sees that the half-width for the metallic branch is about half of the mean doping value, that is $2\sigma_+=0.16$, since the local gap is proportional to the local hole density. As mentioned, the metallic branch distribution has exactly the same form of the STM histogram data of Lang *et al.*,[9] which express the inhomogeneous superconducting regions in Bi2212. For the LSCO system, assuming that it has the same STM/S Gaussian histogram distribution, the optimally doped compound ($\langle\rho\rangle\approx0.16$) must have $2\sigma_+=0.08$. Since the σ_+ values are related with the degree of inhomogeneities, we estimate the σ_+ values for the other compounds using the fact that it decreases with the hole density. Below we show some selected distributions for underdoped, optimally doped, and overdoped compounds.

The density distribution is normalized to unity. For compounds like LSCO, with average densities of $\rho\gg0.25$, that is, in the far overdoped region, we use a single Gaussian distribution which reflects the more homogeneous character of these compounds. For Bi2212, since the optimally doped compound is about twice that of the other families, the single Gaussian distribution is appropriate for compounds with $\rho\gg0.5$. In Sec. III we show how to estimate T_c as function of the local density $\rho(r)$. As already discussed, HTSC compounds are intrinsic inhomogeneous, and each region in the material may have a different superconducting critical temperature $T_c(r)$. The maximum of these temperatures $T_c(r)$ is the pseudogap temperature since it is connected with the opening of the largest gap, that is, the T^* of a given sample with $\langle\rho\rangle$, i.e., $T^*(\langle\rho\rangle)$. Eventually for temperatures below

$T^*(\langle\rho\rangle)$ the regions with local densities between ρ_m and ρ_p become superconducting and the supercurrent may percolate through the sample. Therefore, the local $T_c(\rho_p)$ is the maximum temperature at which a dissipationless current can flow through the system and which is identified as $T_c(\langle\rho\rangle)$, the experimental superconducting critical temperature.

According to the percolation theory, the site percolation threshold occurs in a square lattice when 59% of the sites are filled.[31] Thus we find the density where the hole-rich branch percolates integrating $\int P(\rho)d\rho$ from ρ_m till the integral reaches the value of 0.59, where we define ρ_p. Below $T_c(\langle\rho\rangle)$ the system percolates and, consequently, it is able to hold a dissipationless supercurrent. We should point out that 0.59 is an appropriate value for a single layer cuprate. The site percolation threshold is 0.16 for a simple cubic lattice.[32] Therefore, for a two layer system like Bi2212, the site percolation threshold may be less than 0.59, but since the true value is not known, we will use 0.59 as a first approximation. In Table I, we show some of the parameters used for certain sample and we plot the distribution, as discussed above, in Fig. 2. Notice that Table I and Fig. 2 are for a HTSC system with optimum doping $\langle\rho\rangle \approx 0.16$ like LSCO or YBCO. For Bi2212, the optimum hole doping is about twice this value,[33] and in this case new parameters must be used. Some charge distributions used for the calculations with the Bi2212 family, similar to the ones shown in Fig. 2 above, were also derived.[19]

III. PHASE DIAGRAM

The experimentally based phenomenological charge distribution probability introduced in Sec. II enable us to estimate the appearance of preformed pair at different regions in the crystal provided that we know the onset of superconductivity $T^*[\rho(r)]$. There are several different approaches which can be used to obtain $T^*[\rho(r)]$. We can simply use the *experimental* measured pseudogap temperature $T^* = T^*(\langle\rho\rangle)$ for several different compounds through the identification $T^*[\rho(r)] = T^*(\langle\rho\rangle)$ which is probably the best estimation. Another possibility is perform a theoretical calculation as we have done in the past[37,36] for T_c of a given compound with density $\langle\rho\rangle$ and take $T^*(\rho(r)) = T_c(\langle\rho\rangle)$.

Strictly speaking, due to the nonuniform charge distribution we do not have translational symmetry, and we should use a method which takes the disorder into account.[24,26,27,34,35] However, such theories require the introduction of a phenomenological random potential to simulate the disorder. Since our purpose here is to demonstrate that phase coherence is attained by percolation and it is *independent* of the pairing mechanism, we will take the simplest theoretical approach[37]: we use a BCS-type mean-field approximation in k space on a two-dimensional square lattice with uniform carrier density ρ to estimate the onset temperature of the superconducting d-wave gap, i.e., $T^*(\rho)$. Then we take $T^*[\rho(r)] = T^*(\rho)$ in order to make a map of the superconducting region. We have to bear in mind that this is an approximation but which is worthwhile since it capable to reproduce the experimental T^* values and is reasonable if the size of the grain or stripes domains are larger than the typical pair coherent length. In fact, the latest STM/S results yields grain boundaries of the order of 100–10 nm while the typical coherent lengths are of the order of angstroms. Thus, this approach, with appropriate choice of experimental or calculated parameters, was used before to derive the $T_c(\rho)$ curves[36–38] for some HTSC families, since T_c was, as in normal superconductors, taken as the onset of vanishing gap and ρ was taken as $\langle\rho\rangle$. A two-dimensional extended Hubbard Hamiltonian in a square lattice has been used to model the quasibidimensionality of the carrier motion through the CuO_2 planes,[36–38,40] and is given by

$$H = -\sum_{\langle\langle ij\rangle\rangle\sigma} t_{ij} c^\dagger_{i\sigma} c_{j\sigma} + U\sum_i n_{i\uparrow} n_{i\downarrow} + \sum_{\langle ij\rangle\sigma\sigma'} V_{ij} c^\dagger_{i\sigma} c^\dagger_{j\sigma'} c_{j\sigma'} c_{i\sigma}, \tag{5}$$

where t_{ij} is the nearest-neighbor and next-nearest-neighbor hopping integral between sites i and j; U is the Coulomb on-site correlated repulsion and V_{ij} is the attractive interaction between nearest-neighbor sites i and j. a is the lattice parameter.

Using the well known BCS-type mean-field approximation to develop Eq. (5) in the momentum space, one obtains the self-consistent gap equation, at finite temperatures,[39]

$$\Delta_{\mathbf{k}} = -\sum_{\mathbf{k}'} V_{\mathbf{k}\mathbf{k}'} \frac{\Delta_{\mathbf{k}'}}{2E_{\mathbf{k}'}} \tanh\frac{E_{\mathbf{k}'}}{2k_B T}, \tag{6}$$

with

$$E_{\mathbf{k}} = \sqrt{\varepsilon^2_{\mathbf{k}} + \Delta^2_{\mathbf{k}}}, \tag{7}$$

which contains the dispersion relation $\varepsilon_{\mathbf{k}}$, and the interaction potential $V_{\mathbf{k}\mathbf{k}'}$ which comes from the transformation to the momentum space of Eq. (5).[36,40] In the calculations we have used a dispersion relation derived from the ARPES data[41] with five neighbor hopping integrals. The hopping integrals could also be estimated from band structure calculations.[42] The interaction potential may be given by[36,40]

$$V_{\mathbf{k}\mathbf{k}'} = U + 2V\cos(k_x a)\cos(k'_x a) + 2V\cos(k_y a)\cos(k'_y a). \tag{8}$$

The substitution of Eq. (8) into Eq. (6) leads to appearance of a gap with two distinct symmetries,[36]

$$\Delta_{\mathbf{k}}(T) = \Delta(T)[\cos(k_x a) \pm \cos(k_y a)], \tag{9}$$

where the plus sign is for extended-s wave symmetry and the minus sign for d-wave symmetry. In accordance with Ref. 36 one observes that the d-wave part of the gap do not depend on the coupling constant U, depending only on V. Here we deal only with the d-wave symmetry which is the more accepted pseudogap symmetry.[2]

Using the same BCS-type mean-field approximation, one obtains the hole-content equation[43]

$$\rho(\mu, T) = \frac{1}{2}\sum_{\mathbf{k}} \left(1 - \frac{\varepsilon_{\mathbf{k}}}{E_{\mathbf{k}}} \tanh\frac{E_{\mathbf{k}}}{2k_B T}\right), \tag{10}$$

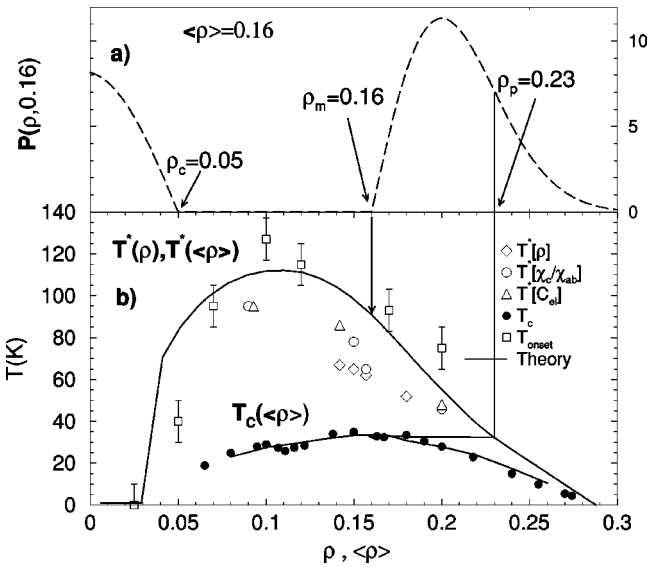

FIG. 3. Phase diagram for the LSCO family. To explain how $T^*(\langle\rho\rangle)$ and $T_c(\langle\rho\rangle)$ are obtained, we plot in (a) the probability distribution for the optimal compound with $\langle\rho\rangle=0.16$, $P(\rho,0.16)$. The arrows shows $T^*(0.16)$ and the percolation threshold at $\rho_p=0.23$ with $T_c(\langle\rho\rangle=0.16)=T_c(0.23)$. The experimental data are taken from Ref. 48 and T_{onset} is taken from the flux flow experiment of Ref. 28 (open squares). Notice that values of $T^*(\langle\rho\rangle)$ are the same of $T_c(\rho)$ but T^* refers to the compound density $\langle\rho\rangle$ and T_c refers to the local density ρ.

where $0\leqslant\rho\leqslant1$.

Equation (10), together with the gap equation (6) must be solved together self-consistently. They may be used to derive the onset of vanishing gap temperature as function of a given value of the density of carriers ρ. This procedure was used in the past to derive, with appropriate set of parameters, the $T_c(\rho)$ phase diagram for different HTSC systems for a single type[36,37,40,44] and for mixture of different order parameter symmetries.[45]

In the present work, we assume a different view, ρ here is not the compound average hole density but the *local* hole density $\rho(r)$. For a given value of $\rho(r)$, we use Eqs. (10) and (6) to calculate the *local* onset temperature of vanishing gap. It is more appropriate to call this temperature $T^*(\rho)$; therefore, $T^*(\rho)\equiv T_c(\rho)$, and hereafter we will deal only with $T^*(\rho)$. On the other hand, the pseudogap temperature of the compound is $T^*(\langle\rho\rangle)=\max\{T_c(\rho)\}$, or simply T^*.

Below, in Fig. 3, we present the results for the $La_{2-x}Sr_xCuO_4$ family. We have used a dispersion relation derived from the Schabel *et al.*[41] In their notation, the hopping parameters are $t\equiv t_1=0.35$eV, $t_2/t_1=0.55$, $t_3/t_1=0.29$, $t_4/t_1=0.19$, and $t_5/t_1=0.06$. The magnitude of the attractive potential was set $V/t=-0.40$ in order to give a reasonable agreement with many measured values of T^*. As we already mentioned, different experiments yield completely different results for T^*. The phase diagram depend on the hopping parameters and on the attractive potential, which is the free parameter in this type of calculation. Thus varying V/t makes the values of the calculated $T^*(\rho)$ change and the position of the optimal density depends on the hopping parameters. The hopping values used below are within the variation estimated by different methods (band structure, ARPES measurement, etc.).[46,47]

The theoretical curves in Fig. 3 are derived in the follow way: For each local density $\rho>\rho_m$, that is, inside the metallic branch, $T^*(\rho)$, calculated with the mean field equations, is a decreasing function. Thus the maximum value of $T^*(\rho)$ is equal to $T^*(\rho_m)$. This is the onset temperature of the superconducting gap (in the metallic branch) and therefore $T^*(\rho_m)=T^*(\langle\rho\rangle)$. To show this, we draw an arrow in Fig. 3 showing how $T^*(\langle\rho\rangle=0.16)$ is obtained. The $T^*(\langle\rho\rangle)$ curve calculated with the above parameter is in good qualitative agreement with the displayed experimental data.[28,48] The value of superconducting critical temperature $T_c(\langle\rho\rangle)$ is estimated in the following manner: we calculate the maximum temperature at which the superconducting region percolates in the metallic branch. This percolation occurs when all the clusters with local density between ρ_m and ρ_p are superconducting. Figure 3(a) shows how this happens for $\langle\rho\rangle=0.16$ which yields $\rho_p=0.23$. This value of ρ_p can be seen in the panel following the arrow, which shows that $T^*(0.23)$ is equal the superconducting critical temperature of the compound, $T_c(\langle0.16\rangle)$. In general $T_c(\langle\rho\rangle)\equiv T^*(\rho_p)$ and the system will be superconducting when submitted to any temperature below $T^*(\rho_p)$ [see Fig. 3(b)]. Below we show the results for the LSCO family. A similar curve was also studied which the T^* is in reasonable agreement with the T_c^{MF} extracted from the high-resolution dilatometry data[49] for $YBa_2Cu_3O_x$.

We have also used this procedure to calculate the phase diagram for the Bi2212 family which is in agreement with the experimental data as it is shown in Fig. 4. The details of the calculations can be found in Ref. 19.

It is worthwhile to mention that the percolating approach is independent of the above mean field calculations for $T^*(\rho)$. It can be used in connection with any method which yields a $T^*(\rho)$ curve. The only requirement is that it would not cross the $T_c(\langle\rho\rangle)$ curve as some have proposed.[16] Thus the percolating approach could be used with some experimental measurements or others theoretical methods to calculate $T^*(\langle\rho\rangle)$, as, for instance, the calculations made with the Hubbard-Holstein Hamiltonian.[50]

IV. DISCUSSION

There are several HTSC phenomena which are not well understood and can be explained with the percolating ideas, and with our model and calculations:

(1) ARPES measurements[3,29] revealed the anomalous behavior of the zero temperature gap $\Delta_0(\langle\rho\rangle)$ which decreases steadily with the doping $\langle\rho\rangle$ although T_c increases by a factor of 2 for their underdoped samples. This overall relation between $\Delta_0(\langle\rho\rangle)$ and T_c is totally unexpected, since it is well known that normal superconductors have a constant value for the ratio $2\Delta_0/k_BT_c$, being 3.75 for usual isotropic order parameter and 4.18 for the $d_{x^2-y^2}$ wave solution.[51]

At low temperatures, since the superconducting phase percolates through different regions, each one has a given $\Delta_0(r)$. Thus tunneling and ARPES experiments detect the

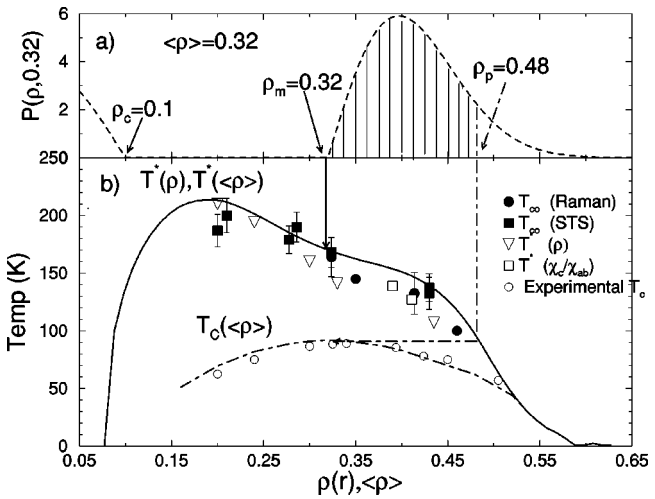

FIG. 4. (a) The probability distribution for the optimal compound with $\langle\rho\rangle = 0.32$. (b) The calculated local onset of the vanishing gap $T^*[\rho(r)]$ and the compound pseudogap temperature $T^*(\langle\rho\rangle)$. The thick arrow shows $T^*(\langle\rho\rangle)$, and the dot-dashed arrow shows how $T_c(\langle\rho\rangle)$ is determined from $T^*(\rho_p)$. The experimental points and the symbols are taking from Ref. 48. Notice that values of $T^*(\langle\rho\rangle)$ refer to the compound average density $\langle\rho\rangle$, and $T^*(\rho)$ refers to the local onset of a vanishing gap at a cluster of density ρ.

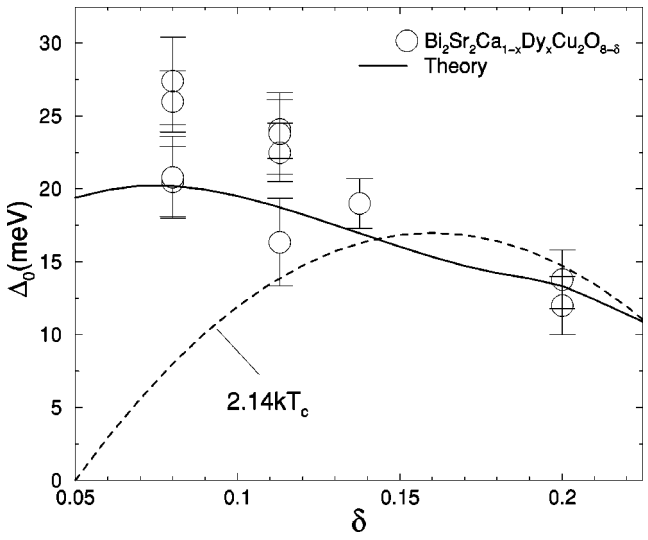

FIG. 5. The zero temperature gap for nine samples as measured by Harris *et al.* (Ref. 29) and our calculations.

largest gap present in the compound. Consequently, $\Delta_0(\langle\rho\rangle)$ must be correlated with the onset of a vanishing gap $T^*(\langle\rho\rangle)$ which is the largest superconducting temperature in the sample, and should not be correlated with $T_c(\langle\rho\rangle)$. As we show in Fig. 5, correlating the values plotted in Fig. 3(b) for $T^*(\langle\rho\rangle)$ with $\Delta_0(\langle\rho\rangle)$, we are able to give a reasonable fit for the data[3,29] on Dy-BSCCO and explains the different energy scales pointed out by several other authors.

(2) Transport experiments have also been used to study the pseudogap.[2] The underdoped and optimum doped high-T_c oxides have a linear behavior for the resistivity in the normal phase up to very high temperatures. However, at T^* there is a deviation from the linear behavior and the resistivity falls faster with decreasing temperature.[2,48] This behavior can be understood by the increasing of superconducting cluster numbers and size, as the temperatures decreases below T^*. Each superconducting cluster produces a short circuit which decreases the resistivity below the linear behavior between T^* and T_c. To obtain a quantitative fitting of this effect, we are presently working on a simulation for the resistivity of a linear metallic medium with short circuited regions which varies with the temperature. The linear behavior of the resistivity above T^* may be also be explained by a percolation procedure. The conductivity of inhomogeneous systems has been considered from different percolative approaches in order to obtain the correct temperature dependence.[32,52] The temperature functional form depends on how the percolation is achieved in the system.

(3) Several measurements made in the presence of a magnetic field seem to agree with the percolating scenario: The magnetotransport measurements[53] in a $La_{2-x}Sr_xCuO_4$ film just above the irreversibility line is in agreement with the notion that the magnetic field penetrates partially in the superconducting regions and destroys some of the superconducting clusters in the film. We have already mentioned the recent measurements of magnetic domains above T_c which has been interpreted as a diamagnetic precursor to the Meissner state, produced by performed pairs in underdoped $La_{2-x}Sr_xCuO_4$ thin films.[20] The existence of superconducting clusters between T^* and T_c easily explains the appearance of local diamagnetic or Meissner domains and, if there is a temperature gradient in the sample, the local flux flows and produces the dynamic flux flow state.[28]

(4) Another important consequence which follows is that the superconducting pairing mechanism should be more easily investigated by experiments performed mainly at T^*. One such experiment was accomplished by Rubio Temprano *et al.*,[54] which measured a large isotope effect associated with T^* and an almost negligible isotopic effect associated with T_c in the slightly underdoped $HoBa_2Cu_4O_8$ compound. The results strongly support the fact that electron-phonon-induced effects are present in the superconducting mechanism associated with T^*. Bussmann-Holder *et al.* also calculated T^* as function of a phonon-induced gap.[55]

In order to gain further insight on the nature of the pair potential, we have measured the resistivity under hydrostatic pressure on an optimally doped $Hg_{0.82}Re_{0.18}Ba_2Ca_2Cu_3O_{8+\delta}$ (Ref. 56) sample. The data indicated a linear increase of T^* with the pressure at the same rate as T_c. In the context of our theory, this result might be in agreement with the phonon induced mechanism: the inhomogeneities local charge densities in a given compound yield varying values for the Fermi level, broadening $N(E_F)$.[24] The applied pressure on a cuprate with an inhomogeneous charge distribution is also expected to broaden the density of states[36] $N(E_F)$, and the main effect of an applied pressure on T_c is an increase of the phonon or Debye frequency. This is seen through a linear increase of T^* (Ref. 56) which also provides a very interesting physical explanation on the origin of the linear pressure induced *intrinsic effect*,[36,57,58] usually postulated to explain the raise of T_c above its maximum value.

(5) The anomalous behavior found mostly in underdoped compounds is related with the temperature behavior of the Hall coefficient[30] R_H and the Hall density n_H which is proportional to the average hole density $\langle\rho\rangle$. While in normal metals n_H is independent of the temperature, in the normal phase of many HTSC, n_H increases monotonically as the temperature increases and saturates at high temperatures.[30,59] This anomalous behavior can be explained by the existence of superconducting islands above T_c which gradually turn into metallic phases as the temperature is raised. Such superconducting regions can be regarded as empty spaces in disordered hole-rich (metallic) and hole-poor (insulator) backgrounds. Therefore, as the metallic region increases, it also increases also the number of carriers. However, we have to point out that the saturation seems to occur near the room temperature, which is much higher than some of the measured values for T^*.

(6) The pseudogap has also been detected through the specific heat coefficient which undergoes changes below T^*. It is well known that the electronic specific heat γ term of the normal phase is a material dependent and temperature independent constant. However, several measurements have detected[2,16,17] a suppression in the γ term in mostly underdoped compounds of different families. In the percolating approach, with the existence of superconducting clusters below T^*, we can qualitatively explain such depression. While the metallic region specific heat behaves as γT, the superconducting region contributes with terms proportional to $\exp(-\Delta(r)/T)$, which decreases much faster with T. As the temperature falls below T^* and the superconducting region increases, its contribution to the specific heat becomes more important and produces the overall downturn in the γ coefficient. For overdoped samples, since T^* is very close T_c, this effect may be difficult to be detected and this is the suppression of the γ term was not seem for overdoped compounds.[16,17]

(7) Magnetization measurements above T_c in oriented powder of $Y_{1-x}Ca_xBa_2Cu_3O_y$ has revealed a pattern[60] which cannot be explained by the usual fluctuation of the magnetization order parameter.[61] Such a pattern was interpreted by the formation of superconducting regions above the percolating threshold,[60] as discussed in detail by the percolating model above. We use the Ginsburg-Landau formalism[61] in connection with the hole charge distribution introduced in Sec. II in order to provide a quantitative calculation for such anomalous induced diamagnetism. The results will be published elsewhere together with a new analysis on the behavior of H_{c2} for high-T_c superconductors.

V. CONCLUSIONS

We have demonstrated that the percolating approach for local preformed pairs due to an inhomogeneous charge distribution on the CuO_2 planes provides a general approach to the phase diagram of the high-T_c cuprate superconductors. The pseudogap is regarded as the largest superconducting gap among the superconducting regions in an inhomogeneous compound. The critical temperature T_c is the maximum temperature at which these superconducting regions percolate. We have shown, through the calculations presented in this paper, that this approach is suitable to reproduce the measured T_c and T^* phase diagrams for several cuprates using a phenomenological real charge distribution drawn from the STM/S data.

One of the advantages of our approach is that the pair formation and the phase coherent superconducting states are studied independently. The phase coherence is attained by percolation. On the other hand, the pair formation was studied by a mean field BCS-like method in order to estimate the onset of superconducting gap T^* for any doping level. This was the simplest method and the calculations could have been done with other theoretical approaches. However, notice that the pair formation mechanism is independent of how the coherent percolative phase is reached. This general approach is in agreement with trends and ideas[26,27] which are based on data and the experimental fact that HTSC's are mostly inhomogeneous materials.

The method developed also provides insights and introduces an interpretation on several typical anomalous properties of HTSC's: these include the dependence of the zero temperature gap $\Delta_0(T)$ on the hole concentration, the downturn of the linear dependence on the resistivity with the temperature, the linear dependence of the hole concentration on the temperature, the suppression of the specific heat coefficient γ, the dependence of T^* on the pressure, and other implications which are presently being studied and which will be discussed in the future.

ACKNOWLEDGMENTS

Financial support of CNPq and FAPERJ is gratefully acknowledged. J.L.G. thanks CLAF for a CLAF/CNPq post doctoral fellowship.

[1] K. Kitazawa, Proceedings of the IV-M2S HTSC conference, [Physica C **341-348**, 19 (2000)].
[2] T. Timusk and B. Statt, Rep. Prog. Phys. **62**, 61 (1999).
[3] C. Renner, B. Revaz, J.-Y Genoud, K. Kadowaki, and O. Fischer, Phys. Rev. Lett. **80**, 149 (1998).
[4] T. Egami and S. J. L. Billinge, in *Physical Properties of High-Temperatures Superconductors V*, edited by D.M. Ginsberg (World Scientific, Singapore, 1996), p. 265.
[5] S. J. L. Billinge, E. S. Bozin, and M. Gutmann, cond-mat/0005032 (unpublished).
[6] E.S. Bozin, G.H. Kwei, H. Takagi, and S.J.L. Billinge, Phys. Rev. Lett. **84**, 5856 (2000).
[7] C. Howald, P. Fournier, and A. Kapitulnik, Phys. Rev. B **64**, 100504 (2001).
[8] S.H. Pan, J.P. ONeal, R.L. Badzey, C. Chamon, H. Ding, J.R. Engelbrecht, Z. Wang, H. Eisaki, S. Uchida, A.K. Gupta, K.W. Ng, E.W. Hudson, K.M. Lang, and J.C. Davis, Nature (London) **413**, 282 (2001); cond-mat/0107347 (unpublished).

[9] K.M. Lang, V. Madhavan, J.E. Hoffman, E.W. Hudson, H. Eisaki, S. Uchida, and J.C. Davis, Nature (London) **415**, 412 (2002).
[10] T. Egami, Proceedings of the New3SC International Conference [Physica C **364-365**, (2001)].
[11] J.M. Traquada, B.J. Sternlieb, J.D. Axe, Y. Nakamura, and S. Uchida, Nature (London) **375**, 561 (1995).
[12] A. Bianconi, N.L. Saini, A. Lanzara, M. Missori, T. Rossetti, H. Oyanagi, H. Yamaguchi, K. Oda, and T. Ito, Phys. Rev. Lett. **76**, 3412 (1996).
[13] V.J. Emery, S.A. Kivelson, and J.M. Traquada, Proc. Natl. Acad. Sci. U.S.A. **96**, 8814 (1999).
[14] M. Randeria, cond-mat/9710223 (unpublished).
[15] V.J. Emery and S.A. Kilvenson, Nature (London) **374**, 434 (1995).
[16] J.L. Tallon and J.W. Loram, Physica C **349**, 53 (2001).
[17] J.W. Loram, K.A. Mirza, J.R. Cooper, and J.L. Tallon, Physica C **282-287**, 1405 (1997).
[18] G.V.M. Williams, J.L. Tallon, J.W. Quilty, H.J. Trodahl, and N.E. Flower, Phys. Rev. Lett. **80**, 377 (1998).
[19] E.V.L. de Mello, E.S. Caixeiro, and J.L. González, cond-mat/0110479 (unpublished), where we made explicity calculations for the Bi system.
[20] I. Iguchi, I. Yamaguchi, and A. Sugimoto, Nature (London) **412**, 420 (2001).
[21] V. Hizhniakov, N. Kistoffel, and E. Sigmund, Physica C **160**, 119 (1989).
[22] R.K. Kremer, E. Sigmund, V. Hizhniakov, F. Hentsch, A. Simon, K.A. Müller, and M. Mehring, Z. Phys. B: Condens. Matter **86**, 319 (1992).
[23] J. Mesot, P. Allenspach, U. Staub, A. Furrer, and H. Mutka, Phys. Rev. Lett. **70**, 865 (1993).
[24] Yu.N. Ovchinnikov, S.A. Wolf, and V.Z. Kresin, Phys. Rev. B **63**, 064524 (2001); Physica C **341-348**, 103 (2000).
[25] D. Mihailovic, V.V. Kabanov, and K.A. Müller, Europhys. Lett. **57**, 254 (2002).
[26] Z. Wang, J.R. Engelbrecht, S. Wang, H. Ding, and S.H. Pan, Phys. Rev. B **65**, 064509 (2002).
[27] J. Burgy, M. Mayr, V. Martin-Mayor, A. Moreo, and E. Dagotto, Phys. Rev. Lett. **87**, 277202 (2002).
[28] Z.A. Xu, N.P. Ong, Y. Wang, T. Kakeshita, and S. Uchida, Nature (London) **406**, 486 (2000).
[29] J.M. Harris, Z.X. Shen, P.J. White, D.S. Marshall, M.C. Schabel, J.N. Eckstein, and I. Bozovic, Phys. Rev. B **54**, R15665 (1996).
[30] N. P. Ong, *Physical Properties of High Temperature Superconductors*, edited by D. M. Ginsberg (World Scientific, Singapore, 1900), Vol. II, p. 459.
[31] D. F. Stauffer and A. Aharony, *Introduction to Percolation Theory* (Taylor & Francis, London, 1994).
[32] G.E. Pike and C.H. Seager, Phys. Rev. B **10**, 1421 (1974).
[33] P. Konsin, N. Kristoffel, and B. Sorkin, J. Phys. C **10**, 6533 (1998).
[34] W.A. Atkinson, P.J. Hirschfeld, and A.H. MacDonald, Phys. Rev. Lett. **85**, 3922 (2001).
[35] Amit Ghosal, Mohit Randeria, and Nandini Trivedi, Phys. Rev. B **65**, 014501 (2002).
[36] G.G.N. Angilella, R. Pucci, and F. Siringo, Phys. Rev. B **54**, 15 471 (1996).
[37] E.V.L. de Mello, Physica C **259**, 109 (1996).
[38] E.V.L. de Mello, Braz. J. Phys. **29**, 551 (1999); Physica B **265**, 142 (1999).
[39] P. G. de Gennes, *Superconductivity of Metals and Alloys* (Benjamin, New York, 1966).
[40] T. Schneider and M.P. Sörensen, Z. Phys. B: Condens. Matter **80**, 331 (1990).
[41] M.C. Schabel, C.-H. Park, A. Matsuura, Z.-X. Shen, D.A. Bonn, X. Liang, and W.N. Hardy, Phys. Rev. B **57**, 6090 (1998).
[42] M.S. Hybertsen, M. Schluter, and N.E. Christensen, Phys. Rev. B **39**, 9028 (1989).
[43] A.J. Leggett, Rev. Mod. Phys. **47**, 331 (1975).
[44] E.S. Caixeiro and E.V.L. de Mello, Physica C **353**, 103 (2001).
[45] E.V.L. de Mello, Physica C **324**, 88 (1999).
[46] R. Raimondi, J.H. Jefferson, and L.F. Feiner, Phys. Rev. B **53**, 8774 (1996).
[47] O.K. Andersen, A.I. Liechtenstein, O. Jepsen, and F. Paulsen, J. Phys. Chem. Solids **56**, 1573 (1995).
[48] M. Oda, N. Momono, and M. Ido, Supercond. Sci. Technol. **13**, R139 (2000).
[49] C. Meingast, V. Pasler, P. Nagel, A. Rykov, S. Tajima, and P. Olsson, Phys. Rev. Lett. **86**, 1606 (2001).
[50] C. Di Castro, M. Grilli, and S. Caprara, cond-mat/0109319 (unpublished).
[51] H. Won and K. Maki, Phys. Rev. B **49**, 1397 (1994).
[52] V. Ambegaokar, B.I. Halperin, and J.S. Langer, Phys. Rev. B **4**, 2612 (1971).
[53] B. Lake, H.M. Rønnow, N.B. Christensen, G. Aeppli, K. Lefmann, D.F. MacMorrow, P. Vorderwisch, P. Smeibidl, N. Mangkorntong, T. Sagawa, M. Nohara, H. Takagi, and T.E. Mason, Science **291**, 759 (2001).
[54] D. Rubio Temprano, J. Mesot, S. Janssen, K. Conder, A. Furrer, H. Mutka, and K.A. Müller, Phys. Rev. Lett. **84**, 1990 (2000).
[55] A. Bussmann-Holder, Alan R. Bishop, H. Büttner, T. Egami, R. Micnas, and K.A. Müller, J. Phys. C **13**, L169 (2001).
[56] E.V.L. de Mello, M.T.D. Orlando, J.L. González, E.S. Caixeiro, and E. Baggio-Saitovitch, Phys. Rev. B **66**, 092504 (2002).
[57] M.T.D. Orlando, A.G Cunha, E.V.L. de Mello, H. Belich, E. Baggio-Saitovitch, A. Sin, X. Obradors, T. Burghardt, and A. Eichler, Phys. Rev. B **61**, 15 454 (2000).
[58] J.L. González, E.S. Yugue, E. Baggio-Saitovitch, M.T.D. Orlando, and E.V.L. de Mello, Phys. Rev. B **63**, 054516 (2001).
[59] Y. Wang and N.P. Ong, cond-mat/0110215 (unpublished).
[60] A. Lascialfari, A. Rigamonti, L. Romano, P. Tedesco, A. Varlamov, and D. Embriaco, Phys. Rev. B **65**, 144523 (2002).
[61] M. Tinkham, *Introduction to Superconductivity* (McGraw-Hill, New York, 1996), Chap. 8.